Journal of NUCLEAR SCIENCE and TECHNOLOGY, Vol. 45, No. 4, p. 313–327 (2008)

ARTICLE

Isotopic Analysis of Actinides and Fission Products in LWR High-Burnup UO_2 Spent Fuels and its Comparison with Nuclide Composition Calculated Using JENDL, ENDF/B, JEF and JEFF

Akihiro SASAHARA[1,*], Tetsuo MATSUMURA[2], Giorgos NICOLAOU[3] and Yoshiaki KIYANAGI[4]

[1]*Nuclear Technology Research Laboratory, Central Research Institute of Electric Power Industry, 2-11-1, Iwado Kita, Komae-Shi, Tokyo 201-8511, Japan*
[2]*Material Science Research Laboratory, Central Research Institute of Electric Power Industry, 2-61 Nagasaka, Yokosuka-Shi, Kanagawa 240-0196, Japan*
[3]*Laboratory of Nuclear Technology, Department of Electrical and Computer Engineering, Faculty of Engineering, Democritus University of Thrace, 67100 Xanthi, Greece*
[4]*Graduate School of Engineering, Hokkaido University, Kita 13, Nishi 8, Kita-ku, Sapporo 060-8628, Japan*

(Received August 24, 2007 and accepted in revised form December 1, 2007)

A chemical isotopic analysis of the actinides and fission products of a high-burnup PWR-UO_2 fuel with an average burnup of 60.2 MWd/kgHM was carried out to accumulate extensive nuclide composition data. Furthermore, computational analysis was performed using the integrated burnup calculation code SWAT. The differences between the amounts obtained by the chemical isotopic analysis and SWAT calculation using JENDL-3.2, JENDL-3.3, ENDF/B-VI.5, ENDF/B-VI.8, JEF-2.2 and JEFF-3.0 were evaluated as the ratios of the calculated values to the experimental values (C/E ratios). For actinides, the calculated ^{244}Cm amount, which is an important nuclide as a major neutron source in spent fuels, was underestimated. The main sensitive path for ^{244}Cm was therefore investigated by a simple depletion calculation for actinides and the cause of the underestimation of the calculated ^{244}Cm amount is discussed. The fission products ^{88}Sr, ^{90}Sr, ^{89}Y, ^{106}Ru, ^{133}Cs, ^{135}Cs and ^{144}Nd, for which the C/E ratios were larger than 1.05 or smaller than 0.95, were investigated to improve their C/E ratios by a simple depletion calculation with simplified burnup chains and sensitivity coefficients, and the correction values for the fission yields or capture cross sections were estimated. The effect of power history on nuclide composition was also investigated. Additionally, the fission products for which the C/E ratios strongly depend on the type of library are discussed using sensitivity coefficients.

KEYWORDS: high-burnup UO_2 fuel, isotopic analysis, actinides, fission products, SWAT code, JENDL-3.2, JENDL-3.3, ENDF/B-VI.5, ENDF/B-VI.8, JEF-2.2, JEFF-3.0, sensitivity analysis

I. Introduction

In the shielding and criticality safety analysis of spent fuel storage facilities, safety evaluation is performed by introducing a safety margin that takes into account such uncertainty in radiation source intensity and its energy distribution from spent fuels, and the reactivity of unirradiated fuel. Radiation source intensity and energy distribution depend on the nuclide composition of spent fuels. Therefore, the verification of and improvement in the accuracy of calculating the nuclide composition in spent fuels are necessary and will lead to a reasonable design as well as to improved shielding and criticality safety analysis of spent fuel storage facilities; they may also contribute to the introduction of burnup credit. This is of particular importance for high-burnup UO_2 spent fuels.

Regarding the experimental determination of nuclide composition, the spent fuel isotopic composition database (SFCOMPO)[1] published by the Nuclear Energy Agency (NEA) includes actinides such as uranium and plutonium isotopes, and some fission products such as cesium and neodymium isotopes in pressurized water reactor (PWR) and boiling water reactor (BWR) spent fuels (UO_2 and UO_2-Gd_2O_3). In the SFCOMPO, the nuclide compositions of Japanese commercial PWR and BWR spent fuels are compiled but their burnups are rather low (~47 MWd/kgHM). In addition, a comparison of the experimental nuclide composition with the calculated one for Japanese commercial spent fuels has been performed using the ratios of the calculated values to the experimental values (C/E ratios).[2,3] Other evaluations of nuclide compositions have been reported in Refs. 4) and 5), in which the trend of the C/E ratios is discussed for UO_2 spent fuels with a burnup range of 30 to 55 MWd/kgHM; however, the experimental nuclide compositions of such fuels have not yet been published.

*Corresponding author, E-mail: sasa@criepi.denken.or.jp

Table 1 Average power histories and burnups for high-burnup PWR-UO_2 fuel

Cycle	Average specific power (MW/t)	Burnup (MWd/kgHM)
1	37.9	11.3
2	48.2	14.9
3	40.6	12.3
4	35.8	11.3
5	32.8	10.4

For source intensity, it has been reported that the calculated neutron intensity emitted by spent fuels is 20–45% lower than the experimental one;[6] this underestimation mainly resulted from the low calculation accuracy of ^{244}Cm that is a major neutron source in spent fuels.

Thus, at present, the experimental nuclide composition data and its evaluation, and discussion for improving the calculation accuracy for the nuclide composition of high-burnup UO_2 spent fuel remain insufficient.

In this study, a chemical isotopic analysis of a high-burnup PWR-UO_2 spent fuel with a burnup range of 53 to 65 MWd/kgHM is carried out to accumulate extensive nuclide composition data for actinides and fission products. Furthermore, computational analysis is carried out using the integrated burnup calculation code system SWAT.[7] The libraries used in this study are JENDL-3.2,[8] JENDL-3.3,[9] ENDF/B-VI.5 (release 6.5), ENDF/B-VI.8 (release 6.8),[10] JEF-2.2[11] and JEFF-3.0,[12] which are generally used in various neutronics codes and adapted for use with SWAT. The differences between the amounts of actinides and fission products obtained by chemical isotopic analysis and calculated by SWAT are evaluated as the C/E ratios.

In actinide isotopes, the ^{244}Cm amount, which directly affects neutron emission by spent fuels after cooling, is investigated on the basis of the C/E ratio using a simple depletion calculation.

For the fission products that are important gamma and decay heat sources, neutron absorbers or burnup indicators and whose C/E ratios are larger than 1.05 or smaller than 0.95, sensitivity analysis is carried out to determine the fission products that strongly influence the production of the concerned fission products and to estimate the correction values for the fission yields or capture cross sections.

The effect of power history on nuclide composition is also investigated. In addition, the fission products for which the C/E ratios strongly depend on the type of library are discussed using sensitivity coefficients.

II. Materials and Methods

1. Specifications of Spent Fuels and Chemical Analysis

The high-burnup PWR-UO_2 spent fuel rod used in this study (3.8% ^{235}U, 60.2 MWd/kgHM declared average burnup) was loaded in a 15 × 15 fuel assembly and irradiated for five cycles in a European commercial nuclear power reactor. Its average power histories and burnups achieved in all cycles are given in **Table 1**.

Table 2 Measurement accuracy for nuclide determination

Nuclide	Measurement accuracy (%)
^{242}Cm, ^{244}Cm	5–10
Ru, ^{134}Cs, ^{137}Cs, ^{144}Ce, ^{154}Eu	3–5
U, Pu	< 0.5
Am, ^{245}Cm, ^{246}Cm, Nd	1
^{147}Pm+^{147}Sm, ^{154}Sm+^{154}Gd	< 3
^{237}Np, Rb, Sr, Y, ^{133}Cs, ^{135}Cs, ^{139}La, ^{140,142}Ce, ^{141}Pr, ^{147}Pm, Sm, ^{153,155}Eu, Gd	2–3

Table 3 Elapsed time from discharge to chemical isotopic analysis for each sample

Sample	Nuclide	Period (day)
A	U, Np, Pu	1206
	Am, Cm, fission products	1234
B, C, D	^{134}Cs, ^{137}Cs, ^{154}Eu	1625
	U, Pu	1649
	Np, other fission products	1696
	Am, Cm	1706

A chemical isotopic analysis of samples A, B, C and D, extracted at four different axial positions of the high-burnup PWR-UO_2 fuel, was carried out. The isotopic composition of sample A has been reported.[13] In the present study, further analysis of samples B, C and D was performed at the Institute for Transuranium Elements (ITU) in Karlsruhe, Germany. In the chemical isotopic analysis, the total dissolution of the samples was performed in nitric acid/hydrogen fluoride solution using an autoclave. Hence, even insoluble isotopes such as ruthenium completely dissolved in the solution.

Each solution from samples B, C and D was analyzed using the following mass- and energy-based spectrometry techniques: thermal ionization mass spectrometry (TIMS), inductively coupled plasma mass spectrometry (ICP-MS), ICP-MS coupled to an ion chromatography column (IC-ICP-MS), and alpha and gamma spectrometry. **Table 2** shows the measurement accuracy for the nuclide determination. These values include the uncertainty in the sample preparation procedure and also in the analytical chemical technique. The elapsed times from the fuel discharge to the chemical isotopic analysis for all the samples are shown in **Table 3**.

2. Computations and Modeling

The nuclide composition of actinides and fission products was computed using the SWAT code, which is an integrated burn-up code developed at the Japan Atomic Energy Research Institute (JAERI). The code contains and combines the general purpose neutronics code SRAC[14] and ORIGEN2.[15] A number of infinite dilution cross sections are prepared in SWAT and can be replaced with the effective

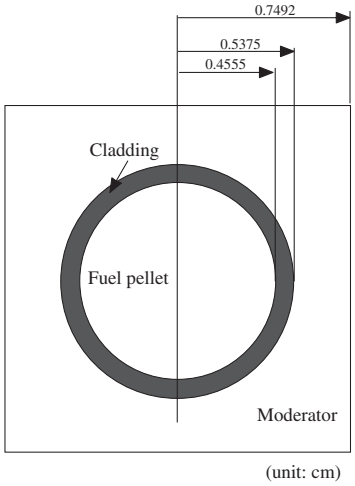

Fig. 1 Dimensions and regions used in calculation for high-burnup PWR-UO_2 fuel

Table 4 Sample burnups determined by chemical isotopic analysis

Sample	Burnup (MWd/kgHM)
A	64.7
B	52.8
C	60.0
D	63.5

cross sections calculated using SRAC. In this study, the neutron spectrum and the effective cross sections were calculated using the ultrafine resonance absorption calculation (PEACO) routine in SRAC, and the effective cross sections for all of the nuclides, which were used to evaluate their C/E ratios were calculated using PEACO. The libraries JENDL-3.2, JENDL-3.3, ENDF/B-VI.5, ENDF/B-VI.8, JEF-2.2 and JEFF-3.0, and the fission yields of JNDC-V2[16] were used in the SWAT calculation.

In a PWR-UO_2 fuel assembly, the homogeneities of the types of fuel and moderator density are better than those in a BWR-UO_2 fuel assembly. Thus, a square cell model was applied, considering an equivalent volume ratio of fuel to moderator with the whole fuel assembly. The geometry used in the calculations is shown in **Fig. 1**. It is composed of three regions: fuel pellet, cladding and moderator. The temperatures of the fuel and cladding were 900 and 600 K, respectively, and they are typical temperatures of LWR fuels. The moderator temperatures for samples A, B, C and D were 591, 568, 596 and 577 K, respectively, and they were calculated by considering the axial power density distribution. The constant boric acid concentration (500 ppm) was used in the calculations.

The uncertainties due to the modeling of the moderator region in the square cell model, temperatures, boron concentration and depletion calculations were estimated and the uncertainty in the calculated results was less than 4%. In SWAT, the neutron flux depending on the depletion is calculated using the SRAC code, which has been verified and is generally used in Japan, and the burnup calculation is carried out using the ORIGEN2 code in which the matrix exponential method is applied. Thus, in the comparison of SWAT with MVP-BURN, which is a continuous-energy Monte Carlo burnup calculation code, the difference in their calculated result is less than 2%.[2]

III. Results and Discussion

1. Nuclide Compositions of Actinides and Fission Products Determined Experimentally

The local burnup was deduced on the basis of both the amounts of the total heavy metals such as uranium and plutonium isotopes, and the amount of ^{148}Nd determined by the chemical isotopic analysis. **Table 4** shows the local burnups for the samples determined by the chemical isotopic analysis. The burnup range of these samples is 53–65 MWd/kgHM.

The isotopic compositions of the following elements were determined: uranium, neptunium, plutonium, americium, curium, rubidium, strontium, yttrium, ruthenium, cesium, lanthanum, cerium, praseodymium, neodymium, promethium, samarium, europium and gadolinium. **Tables 5** shows the number densities per gram solution of the actinides and fission products obtained experimentally. The number density differs between the samples because the weights of the samples dissolved were different. Sample A selected from part of the fuel, in which the highest neutron emission occurred, shows a peak burnup of the fuel. For samples C and D, the chemical isotopic analysis of ^{242}Cm failed because of the low ^{242}Cm concentration. Some of the fission products such as ^{86}Sr and ^{144}Ce were measured only for sample A; for ^{147}Pm and ^{147}Sm, and ^{154}Sm and ^{154}Gd, the sum of their amounts in samples B, C and D was individually measured by ICP-MS.

2. Comparison of Experimental and Computational Compositions

The C/E ratios of the amounts calculated using SWAT to the experimental amounts for actinides and fission products are shown in **Figs. 2** and **3**, respectively. The C/E ratios in the figures are the average of those of samples A, B, C and D for each nuclide. The trend of the C/E ratio for each nuclide was similar among the samples. Thus, the average C/E ratios show the average trend of the calculated amount of each nuclide and were used to investigate the calculated amount of nuclides in the high-burnup UO_2 fuel.

(1) C/E Ratios for Actinides

In Fig. 2(a), the calculated ^{234}U amount is 17–21% larger than the experimental one. The initial ^{234}U amount in fresh fuel strongly depends on the enrichment process for ^{235}U. In this calculation, the overestimation of ^{234}U is most likely caused by the assumed initial amount.

There was scattering in the C/E ratios for ^{237}Np, ^{242m}Am and ^{242}Cm among the samples. In particular, the ^{242m}Am and ^{242}Cm concentrations in the samples are low (Table 5(a)), so that their chemical analysis may be difficult. For ^{237}Np, it is not clear whether the scatter is caused by the difficulty in the chemical analysis process or the calculation accuracy.

Table 5 Results of chemical isotopic analysis of high-burnup PWR-UO_2 spent fuel

(a) Actinides

Nuclide	A[13]	B	C	D	Nuclide	A[13]	B	C	D
	Number/gram solution					Number/gram solution			
^{234}U	8.74×10^{15}	1.14×10^{16}	1.05×10^{16}	9.30×10^{15}	^{242}Pu	1.11×10^{17}	8.73×10^{16}	1.19×10^{17}	1.14×10^{17}
^{235}U	1.64×10^{17}	2.96×10^{17}	2.14×10^{17}	1.60×10^{17}	^{241}Am	2.09×10^{16}	2.31×10^{16}	2.82×10^{16}	3.20×10^{16}
^{236}U	3.66×10^{17}	4.07×10^{17}	4.16×10^{17}	3.88×10^{17}	^{242m}Am	6.48×10^{13}	6.07×10^{13}	8.40×10^{13}	9.60×10^{13}
^{238}U	6.22×10^{19}	7.02×10^{19}	7.11×10^{19}	6.67×10^{19}	^{243}Am	3.01×10^{16}	1.84×10^{16}	3.05×10^{16}	3.80×10^{16}
^{237}Np	5.51×10^{16}	5.70×10^{16}	4.81×10^{16}	5.71×10^{16}	^{242}Cm	1.13×10^{13}	8.40×10^{11}	—	—
^{238}Pu	3.61×10^{16}	2.78×10^{16}	3.97×10^{16}	3.63×10^{16}	^{244}Cm	1.97×10^{16}	9.30×10^{15}	1.62×10^{16}	1.64×10^{16}
^{239}Pu	3.60×10^{17}	3.68×10^{17}	4.00×10^{17}	3.41×10^{17}	^{245}Cm	1.68×10^{15}	6.80×10^{14}	1.40×10^{15}	1.40×10^{15}
^{240}Pu	2.19×10^{17}	2.15×10^{17}	2.45×10^{17}	2.18×10^{17}	^{246}Cm	4.66×10^{14}	1.40×10^{14}	3.80×10^{14}	3.90×10^{14}
^{241}Pu	1.07×10^{17}	9.58×10^{16}	1.12×10^{17}	9.57×10^{16}					

(b) Fission products

Nuclide	A[13]	B	C	D	Nuclide	A[13]	B	C	D
	Number/gram solution ($\times 10^{16}$)					Number/gram solution ($\times 10^{16}$)			
^{85}Rb	4.48	3.09	3.68	3.38	^{146}Nd	15.9	14.8	19.1	16.7
^{87}Rb	9.57	7.10	8.30	7.84	^{148}Nd	7.92	7.21	8.37	8.33
^{86}Sr	0.13	—	—	—	^{150}Nd	4.05	3.50	4.20	4.08
^{88}Sr	13.7	10.9	13.2	12.4	^{147}Pm	0.78	—	—	—
^{90}Sr	17.4	18.6	21.9	20.7	^{147}Sm	2.93	—	—	—
^{89}Y	15.9	15.8	18.2	17.1	^{148}Sm	4.58	3.16	4.90	4.00
^{106}Ru	0.40	—	—	—	^{150}Sm	6.55	5.63	6.70	6.53
^{133}Cs	24.8	28.3	33.8	22.0	^{151}Sm	0.16	—	—	—
^{134}Cs	1.29	0.68	0.94	0.90	^{152}Sm	1.89	1.70	1.90	1.80
^{135}Cs	9.03	8.54	10.7	7.61	^{154}Sm	0.89	—	—	—
^{137}Cs	26.5	23.2	27.5	26.2	^{153}Eu	2.27	2.14	2.60	2.38
^{139}La	20.3	26.7	32.1	29.9	^{154}Eu	0.35	0.30	0.36	0.33
^{140}Ce	30.5	25.8	29.5	27.5	^{155}Eu	0.11	—	—	—
^{142}Ce	26.9	22.8	26.7	25.6	^{154}Gd	0.22	—	—	—
^{144}Ce	0.24	—	—	—	^{155}Gd	0.09	—	—	—
^{141}Pr	21.8	22.9	27.6	24.8	^{156}Gd	4.19	4.34	6.04	6.49
^{142}Nd	0.95	—	—	—	^{158}Gd	0.59	—	—	—
^{143}Nd	12.1	11.9	13.6	12.1	^{160}Gd	0.05	—	—	—
^{144}Nd	34.2	29.7	36.4	36.0	$^{147}Pm+^{147}Sm$	—	4.03	4.24	3.84
^{145}Nd	12.3	12.2	14.0	12.8	$^{154}Sm+^{154}Gd$	—	0.98	1.70	1.22

Hence, more isotopic analysis data for these nuclides in high-burnup UO_2 fuels are necessary for a detailed discussion of their calculation accuracy.

The C/E ratio for ^{241}Am is overestimated (about 15–18%), whereas that for ^{243}Am is underestimated (about 9%). The C/E ratios for ^{245}Cm depend on the libraries but are generally underestimated. The C/E ratios for ^{246}Cm are also underestimated. These trends are similar to those in other evaluations.[2,3]

The neutron intensity, particularly in high-burnup UO_2 spent fuels, is important for the shielding of spent fuel storage facilities. However, the calculated neutron intensity emitted by spent fuels was lower than the experimental one.[6] Curium-244 is the major neutron emission source in spent fuels after a 3∼4-year cooling time, and its major production path in this high-burnup UO_2 fuel is

$$^{238}U \rightarrow {}^{239}Np \rightarrow {}^{239}Pu \rightarrow {}^{240}Pu \rightarrow {}^{241}Pu \rightarrow {}^{242}Pu \rightarrow {}^{243}Pu/{}^{243m}Pu \rightarrow {}^{243}Am \rightarrow {}^{244}Cm.$$

In Fig. 2, the C/E ratios for $^{239\text{-}241}Pu$ are overestimated by 5 to 14% and those for the nuclides from ^{239}Pu to ^{243}Am decrease along this production path; consequently, the C/E ratio for ^{244}Cm calculated with any library is underestimated by 10 to 20%. This trend of C/E ratios is similar to that in the rather low-burnup UO_2 fuels.[2,3] Hence, further discussion of ^{244}Cm production is carried out using the sensitivity coefficients in Section 4.

(2) C/E Ratios for Fission Products

In Fig. 3, the C/E ratios for Sr isotopes, ^{89}Y and ^{144}Ce are underestimated. On the other hand, the C/E ratio for ^{106}Ru is overestimated by about 9%. For cesium isotopes, the C/E ratios for ^{133}Cs and ^{135}Cs are underestimated by about 9%, whereas the calculated amounts of ^{134}Cs and ^{137}Cs are in good agreement with the experimental ones. For neodymium isotopes, generally, their calculated amounts are in good agreement with the experimental ones, except for $^{142\text{-}144}Nd$. The C/E ratio for ^{151}Sm is overestimated by 6 to 13% and that for ^{147}Pm, which is the precursor of samarium isotopes, is also overestimated by about 20%. For gad-

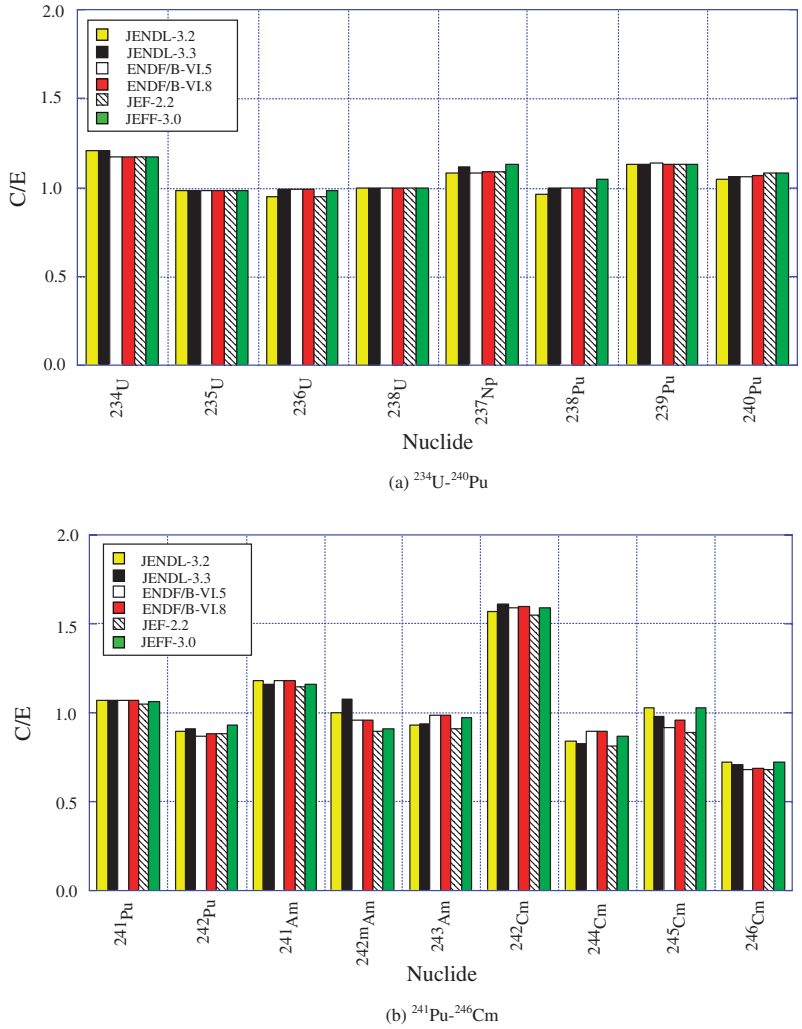

(a) ^{234}U-^{240}Pu

(b) ^{241}Pu-^{246}Cm

Fig. 2 Measured and calculated amounts of actinides as C/E ratio
The C/E ratio for ^{235}U is the depletion ratio between the beginning and end of irradiation; those for other actinides are normalized by the residual ^{238}U amount.

olinium isotopes, generally, their C/E ratios are underestimated.

The C/E ratios for the fission products shown in **Table 6** are not so good, namely, they are greater than 1.05 or less than 0.95 and their calculation accuracy is rather low, although such fission products are important gamma and decay heat sources, neutron absorbers, burnup indicators or are produced in relatively large amounts in spent fuels. Further investigation of the fission products given in Table 6 is therefore carried out using the simplified burnup chains in Section 5.

For ^{154}Eu, ^{155}Eu, ^{154}Gd and ^{155}Gd, their C/E ratios strongly depend on the type of library. Hence, the dependence of the C/E ratios for these fission products on the type of library is discussed in Section 7.

3. Simple Depletion Calculations of Actinides and Fission Products

In the SWAT code, a large number of nuclides can be treated in their burnup calculation. Hence, it is not convenient to focus on particular production paths. For this reason, a simple depletion calculation for actinides and fission products was developed, and production paths that have large sensitivities for concerned nuclides were investigated.

For actinides, the decay and production shown in **Fig. 4** were simplified (Eq. (1)), and the investigation was focused on the ^{244}Cm production path. For fission products, simplified burnup chains, in which the fission yields for short-lived fission product nuclides can be treated as cumulative fission yields, were developed (Eq. (2)) to investigate the production of nuclides shown in Table 6.

- Actinides

$$N_i(t) = N_{i0}exp\{[-(\sigma_{\gamma,il} + \sigma_{f,i})\phi + \lambda_{id}]t\} + \sum_{j=1}^{n} \frac{\sigma_{\gamma,ji}}{\sigma_{\gamma,ji} + \sigma_{f,j}} (N_{j0} - N_j(t)) + \sum_{k=1}^{m} \frac{\lambda_{ki}}{(\sigma_{\gamma,kg} + \sigma_{f,k})\phi + \lambda_{ki}} (N_{k0} - N_k(t)), \quad (1)$$

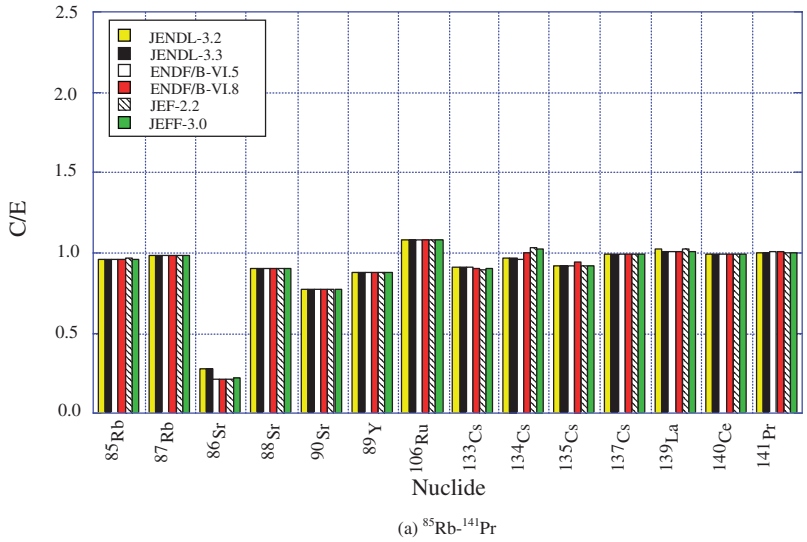

(a) ^{85}Rb-^{141}Pr

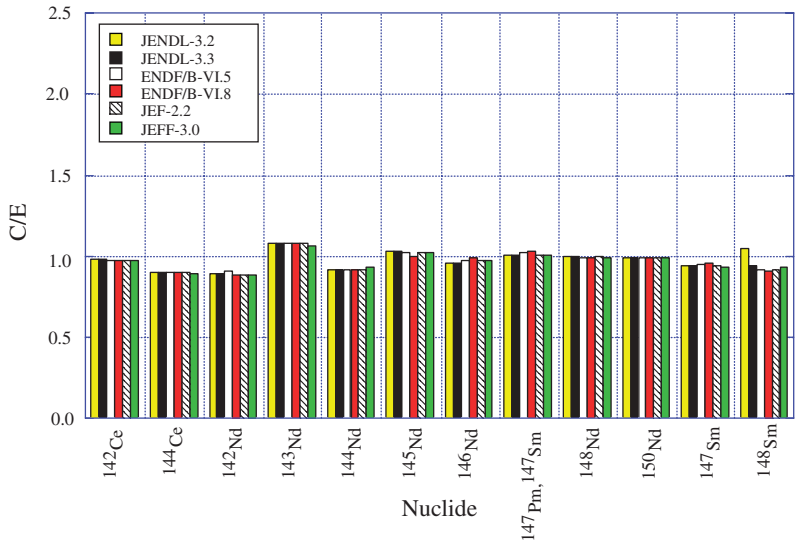

(b) ^{142}Ce-^{148}Sm

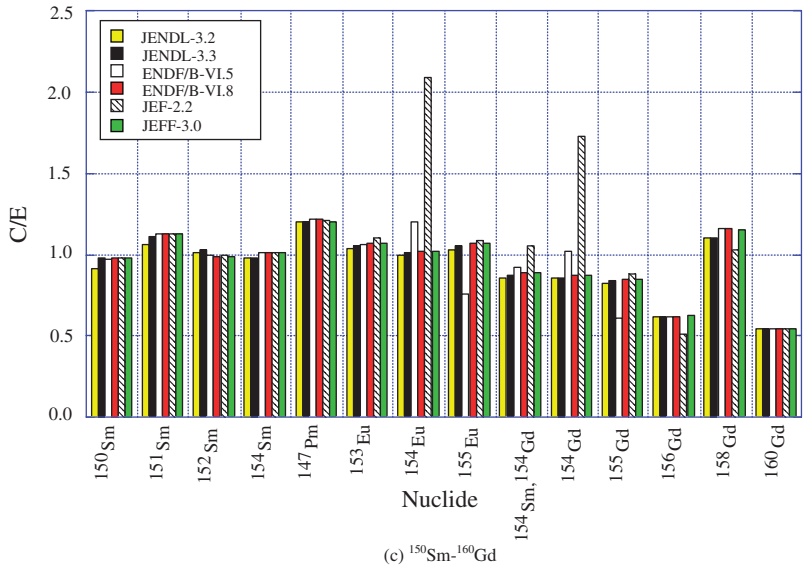

(c) ^{150}Sm-^{160}Gd

Fig. 3 Measured and calculated amounts of fission products as C/E ratio
The C/E ratios are normalized by the residual ^{238}U amount.

Table 6 Fission products investigated

Characteristic	Fission product
Gamma source/decay heat	^{90}Sr
Neutron absorption	^{133}Cs, ^{135}Cs
Burnup indicator	^{106}Ru
Large production amount	^{88}Sr, ^{89}Y, ^{144}Nd

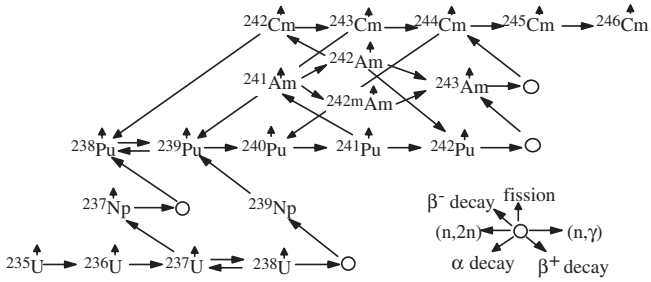

Fig. 4 Depletion chain of actinide

- Fission products

$$\frac{dN_i(t)}{dt} = \gamma_i \Sigma_{f,i}\phi - \sigma_{\gamma,il}N_i(t)\phi + \sigma_{\gamma,ji}N_j(t)\phi - \lambda_{id}N_i(t) + \lambda_{ni}N_n(t), \quad (2)$$

where $N_i(t)$: number density of nuclide i at time = t
N_{i0}: number density of nuclide i at time = 0
$\sigma_{\gamma,il}$: one-group microscopic capture cross section of nuclide i to l
$\sigma_{f,i}$: one-group microscopic fission cross section of nuclide i
λ_{id}: decay constant of nuclide i to d by β^- decay, α decay or isomeric transition
ϕ: one-group neutron flux
$\gamma_i\Sigma_{f,i}$: sum of production from fission reaction of ^{235}U, ^{238}U, ^{239}Pu and ^{241}Pu to nuclide i ($\gamma_i\Sigma_{f,i} = \gamma_{i,U235}\sigma_{f,U235}N_{U235} + \gamma_{i,U238}\sigma_{f,U238}N_{U238} + \gamma_{i,Pu239}\sigma_{f,Pu239}N_{Pu239} + \gamma_{i,Pu241}\sigma_{f,Pu241}N_{Pu241}$)
$\gamma_{i,j}$: fission yield of nuclide j to i.
m, n: numbers of nuclides contributing to decay and capture reaction, respectively.

In Eqs. (1) and (2), one-group microscopic cross sections and neutron flux depending on burnup were previously calculated using SWAT with JENDL-3.3. The number densities N_{U235}, N_{U238}, N_{Pu239} and N_{Pu241} in the term $\gamma_i\Sigma_{f,i}$ of Eq. (2) were also previously calculated using SWAT. The fission yields $\gamma_{i,j}$ were taken from the JNDC-V2 library. In this study, four simplified burnup chains that contain the fission products given in Table 6 were investigated as shown in **Fig. 5**.

The results of the comparison of nuclide compositions between the simple depletion and SWAT calculations are shown in **Table 7**. In the production path for ^{244}Cm, the amounts of uranium, plutonium isotopes and ^{243}Am obtained by the two calculations agree within 4%. The ^{244}Cm amounts agreed within 8%. For fission products that are discussed in the following sections, the two calculations agree within about 3%. Hence, the sensitivity analysis and the correction for the fission yield or capture cross section were carried out using these simple depletion calculations.

Table 7 Differences in amounts of actinides and fission products between simple depletion and SWAT calculations with JENDL-3.3

(a) Actinides

Nuclide	Simple depletion/SWAT
^{238}U	1.00
^{239}Pu	1.04
^{240}Pu	1.02
^{241}Pu	1.03
^{242}Pu	0.98
^{243}Am	0.96
^{244}Cm	0.92

(b) Fission products

Nuclide	Simple depletion/SWAT	Nuclide	Simple depletion/SWAT
^{88}Sr	1.01	^{143}Nd	0.98
^{90}Sr	1.00	^{144}Nd	0.99
^{89}Y	0.99	^{145}Nd	1.00
^{106}Ru	1.01	^{146}Nd	1.00
^{133}Cs	1.00	^{153}Eu	0.97
^{134}Cs	1.00	^{154}Eu	0.97
^{135}Cs	1.00	^{155}Eu	0.97
^{137}Cs	0.99	^{154}Gd	0.97
^{144}Ce	1.00	^{155}Gd	0.97

4. Sensitivity Analysis

A sensitivity analysis was carried out to determine the nuclide that mainly affects the amounts of concerned actinide and fission product using Eqs. (3) and (4)[17] as follows:

$$S_{\sigma_{\alpha,j},N_i} = \frac{\sigma_{\alpha,j}}{N_i}\frac{\Delta N_i}{\Delta\sigma_{\alpha,j}} \quad (3)$$

$$S_{\gamma_{j,k},N_i} = \frac{\gamma_{j,k}}{N_i}\frac{\Delta N_i}{\Delta\gamma_{j,k}}, \quad (4)$$

where $S_{\sigma\alpha,j,Ni}$: sensitivity coefficient of fission or capture cross section of nuclide j to i
$S_{\gamma j,k,Ni}$: sensitivity coefficient of fission yield of nuclide j generated by fission reaction of nuclide k to i
$\sigma_{\alpha,j}$: one-group capture cross section $\sigma_{\gamma,jl}$ or fission cross section $\sigma_{f,j}$ of nuclide j
N_i: number density of nuclide i
$\gamma_{j,k}$: fission yield of nuclide k to j.

In Eqs. (3) and (4), ΔN_i was calculated using Eq. (1) or (2) in which the number density of nuclide i was calculated with a change by 10% in the capture ($\Delta\sigma_{\gamma,jl}$) and fission cross sections ($\Delta\sigma_{f,j}$) of the actinide, and in the capture cross section ($\Delta\sigma_{\gamma,jl}$) and fission yield ($\Delta\gamma_{j,k}$) of the fission product. For actinides, the sensitivity coefficients of all fission and capture cross sections, which are sensitive to ^{244}Cm, are shown in **Table 8**. The decay of actinides during annual

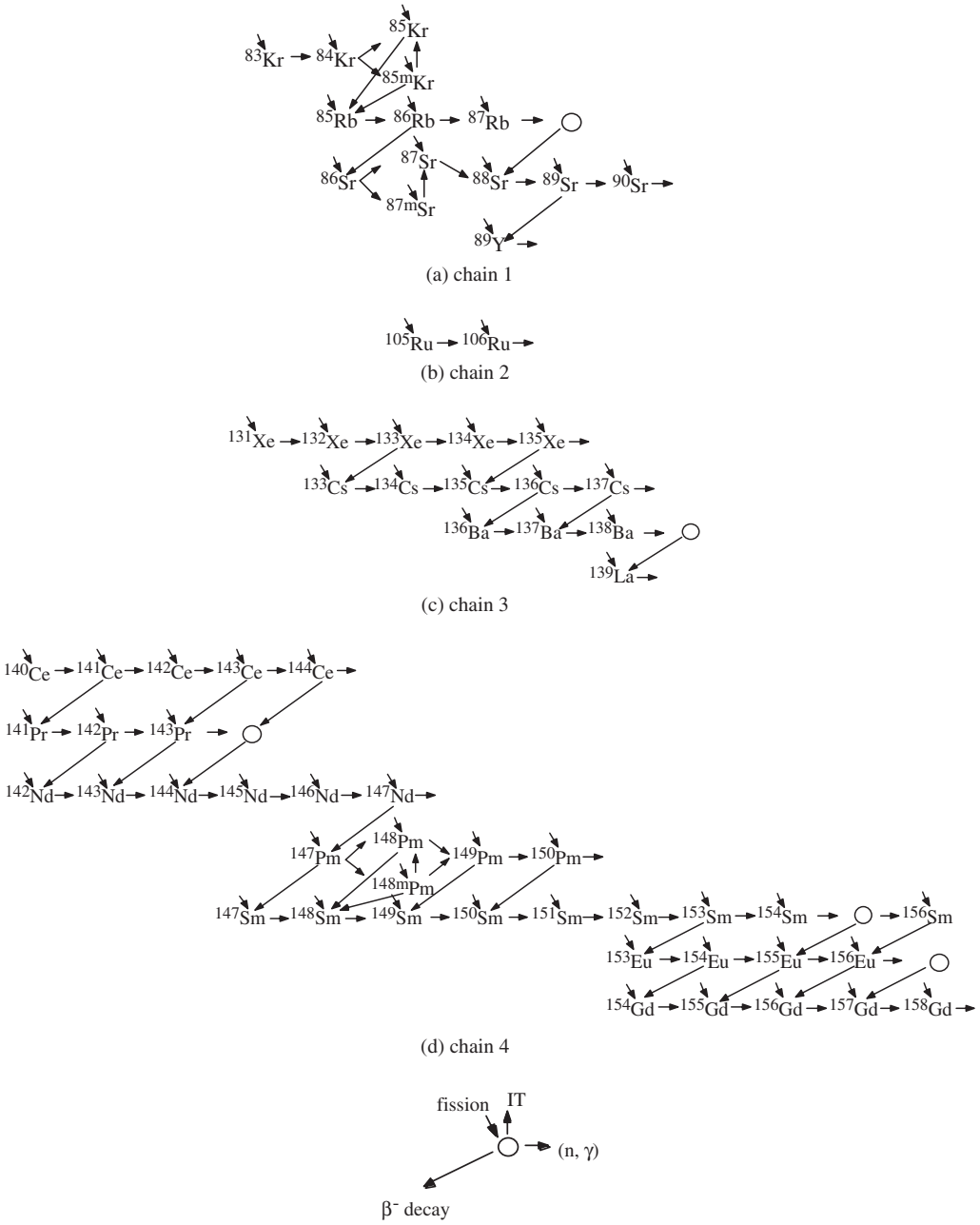

Fig. 5 Depletion chains of fission products

Table 8 Summaries of sensitivity coefficients of fission and capture cross sections of actinides on major production path of ^{244}Cm

	$S_{\sigma\alpha,j,Ni}$									
N_i	$\sigma_{\gamma,238U}$	$\sigma_{f,239Pu}$	$\sigma_{\gamma,239Pu}$	$\sigma_{\gamma,240Pu}$	$\sigma_{f,241Pu}$	$\sigma_{\gamma,241Pu}$	$\sigma_{\gamma,242Pu}$	$\sigma_{\gamma,243Am}$	$\sigma_{f,244Cm}$	$\sigma_{\gamma,244Cm}$
^{238}U	−0.05	0.00	0.00	0.00	0.00	0.00	0.00	0.00	0.00	0.00
^{239}Pu	0.94	−0.58	−0.33	0.00	0.00	0.00	0.00	0.00	0.00	0.00
^{240}Pu	0.96	−0.59	0.63	−0.80	0.00	0.00	0.00	0.00	0.00	0.00
^{241}Pu	0.96	−0.58	0.64	0.14	−0.62	−0.22	0.00	0.00	0.00	0.00
^{242}Pu	0.98	−0.50	0.68	0.25	−0.57	0.76	−0.35	0.00	0.00	0.00
^{243}Am	0.98	−0.45	0.71	0.32	−0.52	0.78	0.68	−0.44	0.00	0.00
^{244}Cm	0.99	−0.40	0.75	0.39	−0.46	0.81	0.73	0.59	−0.01	−0.18

Table 9 Summaries of sensitivity coefficients of fission yields $\gamma_{j,k}$ for fission products

(a) Chain 1

	$S_{\gamma j,k,Ni}$											
	^{88}Sr from				^{89}Sr from				^{90}Sr form			
N_i	^{235}U	^{238}U	^{239}Pu	^{241}Pu	^{235}U	^{238}U	^{239}Pu	^{241}Pu	^{235}U	^{238}U	^{239}Pu	^{241}Pu
^{88}Sr	0.69	0.07	0.20	0.04	0.00	0.00	0.00	0.00	0.00	0.00	0.00	0.00
^{89}Sr	0.00	0.00	0.00	0.00	0.36	0.12	0.41	0.10	0.00	0.00	0.00	0.00
^{90}Sr	0.00	0.00	0.00	0.00	0.00	0.00	0.00	0.00	0.70	0.07	0.20	0.04
^{89}Y	0.00	0.00	0.00	0.00	0.72	0.07	0.19	0.03	0.00	0.00	0.00	0.00

(b) Chain 2

	$S_{\gamma j,k,Ni}$			
	^{106}Ru from			
N_i	^{235}U	^{238}U	^{239}Pu	^{241}Pu
^{106}Ru	0.03	0.07	0.62	0.28

(c) Chain 3

	$S_{\gamma j,k,Ni}$							
	^{133}Xe from				^{135}Xe from			
N_i	^{235}U	^{238}U	^{239}Pu	^{241}Pu	^{235}U	^{238}U	^{239}Pu	^{241}Pu
^{133}Xe	0.15	0.10	0.55	0.19	0.00	0.00	0.00	0.00
^{135}Xe	0.00	0.00	0.00	0.00	0.14	0.09	0.57	0.19
^{133}Cs	0.43	0.08	0.39	0.10	0.00	0.00	0.00	0.00
^{134}Cs	0.52	0.07	0.33	0.07	0.00	0.00	0.00	0.00
^{135}Cs	0.07	0.01	0.03	0.00	0.40	0.07	0.34	0.08
^{137}Cs	0.00	0.00	0.00	0.00	0.00	0.00	0.00	0.00

(d) Chain 4

	$S_{\gamma j,k,Ni}$																			
	^{143}Ce from				^{144}Ce from				^{147}Nd from				^{149}Pm from				^{151}Sm from			
N_i	^{235}U	^{238}U	^{239}Pu	^{241}Pu	^{235}U	^{238}U	^{239}Pu	^{241}Pu	^{235}U	^{238}U	^{239}Pu	^{241}Pu	^{235}U	^{238}U	^{239}Pu	^{241}Pu	^{235}U	^{238}U	^{239}Pu	^{241}Pu
^{143}Ce	0.19	0.10	0.51	0.19	0.00	0.00	0.00	0.00	0.00	0.00	0.00	0.00	0.00	0.00	0.00	0.00	0.00	0.00	0.00	0.00
^{144}Ce	0.00	0.00	0.00	0.00	0.34	0.10	0.42	0.15	0.00	0.00	0.00	0.00	0.00	0.00	0.00	0.00	0.00	0.00	0.00	0.00
^{143}Pr	0.20	0.10	0.51	0.19	0.00	0.00	0.00	0.00	0.00	0.00	0.00	0.00	0.00	0.00	0.00	0.00	0.00	0.00	0.00	0.00
^{143}Nd	0.47	0.07	0.35	0.10	0.00	0.00	0.00	0.00	0.00	0.00	0.00	0.00	0.00	0.00	0.00	0.00	0.00	0.00	0.00	0.00
^{144}Nd	0.23	0.02	0.09	0.02	0.38	0.05	0.16	0.04	0.00	0.00	0.00	0.00	0.00	0.00	0.00	0.00	0.00	0.00	0.00	0.00
^{151}Sm	0.00	0.00	0.00	0.00	0.00	0.00	0.00	0.00	0.07	0.01	0.04	0.01	0.15	0.04	0.14	0.04	0.06	0.06	0.29	0.13
^{152}Sm	0.00	0.00	0.00	0.00	0.00	0.00	0.00	0.00	0.04	0.01	0.02	0.00	0.11	0.02	0.08	0.02	0.08	0.05	0.22	0.08
^{153}Sm	0.00	0.00	0.00	0.00	0.00	0.00	0.00	0.00	0.04	0.00	0.02	0.00	0.09	0.02	0.06	0.02	0.07	0.04	0.18	0.07
^{153}Eu	0.00	0.00	0.00	0.00	0.00	0.00	0.00	0.00	0.03	0.00	0.01	0.00	0.08	0.01	0.04	0.01	0.11	0.04	0.17	0.05
^{154}Eu	0.00	0.00	0.00	0.00	0.00	0.00	0.00	0.00	0.02	0.00	0.01	0.00	0.07	0.01	0.04	0.01	0.12	0.04	0.17	0.05
^{155}Eu	0.00	0.00	0.00	0.00	0.00	0.00	0.00	0.00	0.02	0.00	0.01	0.00	0.07	0.01	0.03	0.01	0.11	0.03	0.15	0.04
^{154}Gd	0.00	0.00	0.00	0.00	0.00	0.00	0.00	0.00	0.01	0.00	0.00	0.00	0.05	0.01	0.02	0.00	0.16	0.04	0.13	0.03
^{155}Gd	0.00	0.00	0.00	0.00	0.00	0.00	0.00	0.00	0.02	0.00	0.01	0.00	0.06	0.01	0.03	0.01	0.13	0.04	0.14	0.04

(to be continued on next page)

inspection was considered in estimating the sensitivity coefficients. For fission products, the sensitivity coefficients of all the fission yields and capture cross sections, which are sensitive to fission products in relation to discussions in the following sections, are shown in **Tables 9** and **10**, respectively. The main results obtained from the sensitivity analysis are described as follows.

(1) Production of ^{244}Cm

In Table 8, the ^{244}Cm amount is highly sensitive to the fission and/or capture cross sections of ^{238}U, $^{239\text{-}242}$Pu and ^{243}Am as well as to the ^{244}Cm capture cross section. In Ref. 18), it has been reported that the measured effective capture cross section for ^{243}Am is 16.3% greater than that calculated with JENDL-3.3. In Fig. 2, the calculated amounts of ^{240}Pu and ^{241}Pu were overestimated by 5~7%. In addition, the sensitivity coefficients of their capture cross sections for the ^{244}Cm amount are also large as shown in Table 8. Therefore, for example, the following three cases in which the capture cross sections of not only ^{243}Am but also plutonium isotopes were adjusted were investigated to improve the calculated ^{244}Cm amount, taking account of the sensitivity coefficients for ^{244}Cm and the trend of the

(e) Chain 4 (cont.)

	$S_{\gamma j,k,Ni}$															
	^{152}Sm from				^{153}Sm from				^{154}Sm from				^{155}Eu from			
N_i	^{235}U	^{238}U	^{239}Pu	^{241}Pu	^{235}U	^{238}U	^{239}Pu	^{241}Pu	^{235}U	^{238}U	^{239}Pu	^{241}Pu	^{235}U	^{238}U	^{239}Pu	^{241}Pu
^{143}Ce	0.19	0.10	0.51	0.19	0.00	0.00	0.00	0.00	0.00	0.00	0.00	0.00	0.00	0.00	0.00	0.00
^{144}Ce	0.00	0.00	0.00	0.00	0.00	0.00	0.00	0.00	0.00	0.00	0.00	0.00	0.00	0.00	0.00	0.00
^{143}Pr	0.00	0.00	0.00	0.00	0.00	0.00	0.00	0.00	0.00	0.00	0.00	0.00	0.00	0.00	0.00	0.00
^{143}Nd	0.00	0.00	0.00	0.00	0.00	0.00	0.00	0.00	0.00	0.00	0.00	0.00	0.00	0.00	0.00	0.00
^{144}Nd	0.00	0.00	0.00	0.00	0.00	0.00	0.00	0.00	0.00	0.00	0.00	0.00	0.00	0.00	0.00	0.00
^{151}Sm	0.01	0.01	0.01	0.01	0.00	0.00	0.00	0.00	0.00	0.00	0.00	0.00	0.00	0.00	0.00	0.00
^{152}Sm	0.05	0.03	0.16	0.07	0.00	0.00	0.00	0.00	0.00	0.00	0.00	0.00	0.00	0.00	0.00	0.00
^{153}Sm	0.04	0.03	0.13	0.06	0.01	0.02	0.09	0.05	0.00	0.00	0.00	0.00	0.00	0.00	0.00	0.00
^{153}Eu	0.07	0.03	0.13	0.04	0.03	0.02	0.10	0.05	0.00	0.00	0.00	0.00	0.00	0.00	0.00	0.00
^{154}Eu	0.07	0.03	0.13	0.04	0.04	0.02	0.10	0.04	0.00	0.00	0.00	0.00	0.00	0.00	0.00	0.00
^{155}Eu	0.07	0.02	0.11	0.03	0.04	0.02	0.09	0.04	0.00	0.00	0.01	0.00	0.00	0.01	0.05	0.03
^{154}Gd	0.11	0.03	0.11	0.02	0.09	0.03	0.12	0.04	0.00	0.00	0.00	0.00	0.00	0.00	0.00	0.00
^{155}Gd	0.08	0.02	0.11	0.03	0.05	0.02	0.10	0.04	0.00	0.00	0.00	0.00	0.00	0.01	0.04	0.02

Table 10 Summaries of sensitivity coefficients of capture cross sections $\sigma_{\gamma,j}$ for fission products

(a) Chain 3

	$S_{\sigma\gamma,j,Ni}$				
			$\sigma_{\gamma,j}$ of		
N_i	^{132}Xe	^{135}Xe	^{133}Cs	^{134}Cs	^{135}Cs
^{133}Xe	0.01	0.00	0.00	0.00	0.00
^{135}Xe	0.00	−0.73	0.00	0.00	0.00
^{133}Cs	0.00	0.00	−0.24	0.00	0.00
^{134}Cs	0.00	0.00	0.80	−0.15	0.00
^{135}Cs	0.00	−0.62	0.09	0.10	−0.06
^{137}Cs	0.00	0.00	0.00	0.00	0.00

(b) Chain 4

	$S_{\sigma\gamma,j,Ni}$															
								$\sigma_{\gamma,j}$ of								
N_i	^{143}Nd	^{144}Nd	^{147}Pm	^{148m}Pm	^{148}Pm	^{148}Sm	^{149}Sm	^{150}Sm	^{151}Sm	^{152}Sm	^{154}Sm	^{153}Eu	^{154}Eu	^{155}Eu	^{154}Gd	^{155}Gd
^{143}Ce	0.00	0.00	0.00	0.00	0.00	0.00	0.00	0.00	0.00	0.00	0.00	0.00	0.00	0.00	0.00	0.00
^{144}Ce	0.00	0.00	0.00	0.00	0.00	0.00	0.00	0.00	0.00	0.00	0.00	0.00	0.00	0.00	0.00	0.00
^{143}Pr	0.00	0.00	0.00	0.00	0.00	0.00	0.00	0.00	0.00	0.00	0.00	0.00	0.00	0.00	0.00	0.00
^{143}Nd	−0.50	0.00	0.00	0.00	0.00	0.00	0.00	0.00	0.00	0.00	0.00	0.00	0.00	0.00	0.00	0.00
^{144}Nd	0.24	−0.01	0.00	0.00	0.00	0.00	0.00	0.00	0.00	0.00	0.00	0.00	0.00	0.00	0.00	0.00
^{151}Sm	0.00	0.00	0.06	0.01	0.01	0.01	−0.01	0.38	−0.90	0.00	0.00	0.00	0.00	0.00	0.00	0.00
^{152}Sm	0.00	0.00	0.04	0.01	0.00	0.00	−0.01	0.25	0.01	−0.78	0.00	0.00	0.00	0.00	0.00	0.00
^{153}Sm	0.00	0.00	0.03	0.01	0.00	0.00	0.00	0.20	0.01	−0.45	0.00	0.00	0.00	0.00	0.00	0.00
^{153}Eu	0.00	0.00	0.02	0.00	0.00	0.00	0.00	0.16	0.01	−0.36	0.00	−0.63	0.00	0.00	0.00	0.00
^{154}Eu	0.00	0.00	0.02	0.00	0.00	0.00	0.00	0.15	0.02	−0.34	0.00	0.33	−0.83	0.00	0.00	0.00
^{155}Eu	0.00	0.00	0.02	0.00	0.00	0.00	0.00	0.13	0.02	−0.29	0.01	0.31	0.08	−0.88	0.00	0.00
^{154}Gd	0.00	0.00	0.01	0.00	0.00	0.00	0.00	0.10	0.03	−0.22	0.00	0.49	−0.76	0.00	−0.15	0.00
^{155}Gd	0.00	0.00	0.02	0.00	0.00	0.00	0.00	0.12	0.02	−0.27	0.01	0.36	−0.14	−0.64	0.22	−0.90

C/E ratios shown in Fig. 2.

- Case 1: The capture cross section of ^{243}Am increases by 16.3%.
- Case 2: The capture cross sections of ^{243}Am and ^{241}Pu increase by 16.3 and 5%, respectively.
- Case 3: The capture cross sections of ^{243}Am, ^{240}Pu and ^{241}Pu increase by 16.3, 5 and 5%, respectively.

In the three cases calculated using Eq. (1), the ^{244}Cm amount was increased by 9.2, 13.6 and 15.8% (**Table 11**), respectively, by adjusting the capture cross sections for ^{243}Am and plutonium isotopes; consequently, the C/E ratio for ^{244}Cm calculated with JENDL-3.3 improved from 0.83 to 0.88, 0.92 and 0.94, respectively. From the results, although the reevaluation of the cross sections is necessary

Table 11 Changes in amounts of ^{240}Pu, ^{241}Pu, ^{242}Pu, ^{243}Am and ^{244}Cm after adjustment

	Before adjustment	After adjustment (Change in amount) (%)		
Nuclide	C/E	Case 1	Case 2	Case 3
^{240}Pu	1.06	0.1	0.1	−3.9
^{241}Pu	1.07	0.0	−1.1	−0.4
^{242}Pu	0.91	0.0	3.9	5.2
^{243}Am	0.94	−6.9	−3.3	−1.7
^{244}Cm	0.83	9.2	13.6	15.8

for the comprehensive discussion based on further experimental results and their evaluations, the calculation accuracy of ^{244}Cm will be improved by the reevaluating the capture cross sections of ^{243}Am and plutonium isotopes, and finally, that of the neutrons emitted from spent fuels will also be improved.

(2) Production of ^{135}Cs and ^{144}Nd

In the cases of ^{135}Cs and ^{144}Nd, which are discussed in Section 5, there are two individual paths that have high sensitivities to their amounts as follows:

- ^{135}Cs: ^{133}Xe → ^{133}Cs → ^{134}Cs → ^{135}Cs and ^{135}Xe → ^{135}Cs,
- ^{144}Nd: ^{143}Ce → ^{143}Pr → ^{143}Nd → ^{144}Nd and ^{144}Ce → ^{144}Nd.

For both nuclides, the latter paths are clearly the main sensitive paths.

(3) Production of ^{154}Eu, ^{154}Gd, ^{155}Eu and ^{155}Gd

In the cases of ^{154}Eu, ^{154}Gd, ^{155}Eu and ^{155}Gd, which are discussed in Section 7, the paths that have large sensitivities to their amounts are

- ^{151}Sm → ^{152}Sm → ^{153}Sm → ^{153}Eu → ^{154}Eu → ^{154}Gd → ^{155}Gd,
- ^{151}Sm → ^{152}Sm → ^{153}Sm → ^{153}Eu → ^{154}Eu → ^{155}Eu → ^{155}Gd.

In Table 10(b), the sensitivity coefficient of the capture cross section of ^{155}Eu for the ^{155}Gd amount is −0.64, while that of ^{154}Gd for ^{155}Gd is 0.22. Thus, the amount of ^{155}Gd strongly depends on that of ^{155}Eu rather than on that of ^{154}Gd. From this result, the main sensitive path for ^{155}Gd is the latter one.

5. Correction of Fission Yield or Capture Cross Section based on Sensitivity Analysis

To improve the calculation accuracy, the fission yield or capture cross section of the fission product that strongly affects the nuclide shown in Table 6 was corrected by making the C/E ratio for the concerned fission product equal to unity using Eq. (3) or (4). Namely, the correction value for the fission yield or capture cross section was defined using Eq. (5), and estimated with the C/E ratios shown in Fig. 3 and the sensitivity coefficients shown in Tables 9 and 10. Additionally, the recalculation using Eq. (2) with the correction value was performed to estimate the C/E ratio for the concerned nuclide.

$$\frac{R_{0,j} - R_j}{R_j} = \frac{1}{S_{j,i}} \left(\frac{1}{(C/E)_i} - 1 \right), \tag{5}$$

where $R_{0,j}$: corrected fission yield or capture cross section of nuclide j
R_j: fission yield $\gamma_{j,k}$ or capture cross section $\sigma_{\gamma,jl}$ of nuclide j before correction
$S_{j,i}$: sensitivity coefficient $S_{\sigma\gamma,j,Ni}$ or $S_{\gamma j,k,Ni}$
$(C/E)_i$: C/E ratio for nuclide i before correction.

Table 12 C/E ratios for ^{88}Sr with correction

	Before correction	Correction for fission yield
		^{88}Sr +11%
Ni	C/E	C/E
^{88}Sr	0.90	1.00
^{90}Sr	0.77	0.77
^{89}Y	0.87	0.87

Table 13 C/E ratios for ^{90}Sr with correction

	Before correction	Correction for fission yield
		^{90}Sr +30%
Ni	C/E	C/E
^{90}Sr	0.77	1.00

In the following, the correction value and C/E ratio for each nuclide were discussed. Here the *S*'s in parentheses are the sum of the sensitivity coefficients for the fission yields of ^{235}U, ^{238}U, ^{239}Pu and ^{241}Pu in Table 9 or the sensitivity coefficient for the capture cross section in Table 10.

(1) ^{88}Sr and ^{90}Sr

The C/E ratios for ^{88}Sr and ^{90}Sr are 0.90 and 0.77, respectively. The amounts of ^{88}Sr and ^{90}Sr are sensitive only to their own fission yields ($S = 1.00$ for ^{88}Sr and ^{90}Sr, respectively); they are not sensitive to the fission yields or capture cross sections of the other fission products in chain 1. This indicates that the underestimation of the amounts of these two fission products results from the underestimation of their own fission yields. Thus, a correction was performed on the fission yield of both fission products. The correction value of +11% for the ^{88}Sr fission yield was estimated using Eq. (5); consequently, the C/E ratio for ^{88}Sr improved from 0.90 to 1.00 (**Table 12**).

Similarly, for ^{90}Sr, the correction value of its own fission yield was +30% and its C/E ratio obtained by recalculation improved from 0.77 to 1.00 (**Table 13**). The two corrections did not affect the C/E ratios for the other fission products in chain 1.

(2) ^{89}Y

The C/E ratio for ^{89}Y is 0.87. The ^{89}Y amount is sensitive only to the ^{89}Sr fission yield ($S = 1.00$) because ^{89}Y is

Table 14 C/E ratios for ^{89}Y with correction

	Before correction	Correction for fission yield
		^{89}Sr +15%
Ni	C/E	C/E
^{90}Sr	0.77	0.77
^{89}Y	0.87	1.00

Table 15 C/E ratios for ^{106}Ru with correction

	Before correction	Correction for fission yield
		^{106}Ru −8%
Ni	C/E	C/E
^{106}Ru	1.09	1.00

Table 16 C/E ratios for ^{133}Cs with correction

	Before correction	Correction for fission yield	Correction for capture cross section
		^{133}Xe +10%	^{133}Cs −41%
Ni	C/E	C/E	C/E
^{133}Cs	0.91	1.00	1.01
^{134}Cs	0.97	1.07	0.62
^{135}Cs	0.92	0.93	0.88
^{137}Cs	0.99	0.99	0.99

Table 17 C/E ratios for ^{135}Cs with correction

	Before correction	Correction for fission yield		Correction for capture cross section			
		^{133}Xe +79%	^{135}Xe +10%	^{135}Xe −14%	^{133}Cs +93%	^{134}Cs +91%	^{135}Cs −100%
Ni	C/E	C/E	C/E	C/E	C/E	C/E	C/E
^{133}Cs	0.91	1.63	0.91	0.91	0.73	0.91	0.91
^{134}Cs	0.97	1.73	0.97	0.97	1.59	0.85	0.97
^{135}Cs	0.92	1.00	1.00	1.01	0.99	0.99	0.96
^{137}Cs	0.99	0.99	0.99	0.99	0.99	0.99	0.99

mainly generated through the β^- decay of ^{89}Sr. Therefore, this indicates that the underestimation of the calculated ^{89}Y amount results from the underestimation of the ^{89}Sr fission yield. The correction value for the fission yield of ^{89}Sr was +15%; consequently, the C/E ratio for ^{89}Y improved from 0.87 to 1.00 with the correction (**Table 14**).

(3) ^{106}Ru

The C/E ratio for ^{106}Ru is 1.09. The ^{106}Ru amount is sensitive only to ^{106}Ru's own fission yield ($S = 1.00$). Therefore, the overestimation of the calculated ^{106}Ru amount results from the overestimation of its own fission yield. The C/E ratio for ^{106}Ru improved from 1.09 to 1.00 (**Table 15**) by using the correction value of −8% for its own fission yield.

(4) ^{133}Cs

The C/E ratio for ^{133}Cs is 0.91. The ^{133}Cs amount is highly sensitive to the ^{133}Xe fission yield ($S = 1.00$) and the ^{133}Cs capture cross section ($S = -0.24$). Thus, a correction was carried out on the fission yield or capture cross section of ^{133}Xe and ^{133}Cs. The results obtained by recalculations are shown in **Table 16**. The correction value of −41% for the ^{133}Cs capture cross section improved the C/E ratio for ^{133}Cs from 0.91 to 1.01. However, the C/E ratios for ^{134}Cs and ^{135}Cs then decreased from 0.97 to 0.62 and from 0.92 to 0.88, respectively. On the other hand, the correction value of +10% for the ^{133}Xe fission yield improved the C/E ratio for ^{133}Cs from 0.91 to 1.00. Then, the C/E ratios for ^{134}Cs and ^{135}Cs increased from 0.97 to 1.07 and from 0.92 to 0.93, respectively. Considering the trend of the C/E ratios for ^{134}Cs and ^{135}Cs, the results suggest that the underestimation of the calculated ^{133}Cs amount is mainly caused by the underestimation of the ^{133}Xe fission yield.

(5) ^{135}Cs

The C/E ratio for ^{135}Cs is 0.92. The ^{135}Cs amount is sensitive to the fission yields of ^{133}Xe ($S = 0.11$) and ^{135}Xe ($S = 0.89$), and the capture cross sections of ^{135}Xe ($S = -0.62$), ^{133}Cs ($S = 0.09$), ^{134}Cs ($S = 0.10$) and ^{135}Cs ($S = -0.06$). The correction for the fission yield or capture cross section was performed and the results of recalculations are shown in **Table 17**. The correction value of +93% for the ^{133}Cs capture cross section resulted in the further underestimation of its own calculated amount; however, the calculated ^{134}Cs amount was overestimated. On the other hand, the correction value of +91% for the ^{134}Cs capture cross section resulted in the underestimation of ^{134}Cs's own calculated amount. From the two corrections, it is thought that the

Table 18 C/E ratios for ^{144}Nd with correction

	Before correction	Correction for fission yield		Correction for capture cross section
		^{143}Ce +27%	^{144}Ce +16%	^{143}Nd +41%
Ni	C/E	C/E	C/E	C/E
^{144}Ce	0.90	0.90	1.04	0.90
^{143}Nd	1.05	1.34	1.05	0.86
^{144}Nd	0.91	0.99	1.01	0.98
^{145}Nd	1.03	1.03	1.04	1.03
^{146}Nd	0.96	0.96	0.96	0.96

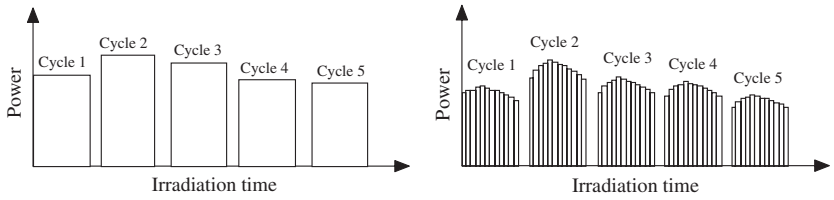

(a) Constant power history (b) Detailed power history

Fig. 6 Scheme of power histories

underestimation of the calculated ^{135}Cs amount is not caused by the capture cross section of ^{133}Cs or ^{134}Cs. Regarding xenon isotopes, for the correction value of +79% for the ^{133}Xe fission yield, the calculated amounts of ^{133}Cs and ^{134}Cs were markedly overestimated. The correction value of +10% for the ^{135}Xe fission yield resulted in a C/E ratio of 1.00 for ^{135}Cs, and that of −14% for the ^{135}Xe capture cross section resulted in a C/E ratio of 1.01. Additionally, the correction for the fission yield or capture cross section of ^{135}Xe negligibly affected the calculated amounts of the other nuclides. For the ^{135}Cs capture cross section, its sensitivity coefficient is small. Thus, the C/E ratio improved from 0.92 to 0.96 when the capture cross section of ^{135}Cs was close to zero (*i.e.*, the correction value was nearly −100%). The trends of the C/E ratios as mentioned above suggest that the underestimation of the fission yield or the overestimation of the capture cross section of ^{135}Xe results mainly in the underestimation of the calculated ^{135}Cs amount.

(6) ^{144}Nd

The C/E ratio for ^{144}Nd is 0.91. The ^{144}Nd amount is highly sensitive to the fission yields of ^{143}Ce (S = 0.36) and ^{144}Ce (S = 0.63), and the capture cross section of ^{143}Nd (S = 0.24). The results from recalculations with correction are given in **Table 18**. The correction value of +27% for the ^{143}Ce fission yield resulted in a C/E ratio of 1.34 for ^{143}Nd. Although the correction value of +41% for the ^{143}Nd capture cross section resulted in a C/E ratio of 0.98 for ^{144}Nd, the C/E ratio for ^{143}Nd decreased from 1.05 to 0.86. On the other hand, the correction value of +16% for the ^{144}Ce fission yield improved the C/E ratio for ^{144}Nd from 0.91 to 1.01 and this correction hardly affected the C/E ratios for the other nuclides. The results suggest that the underestimation of the ^{144}Ce fission yield results mainly in the underestimation of the calculated ^{144}Nd amount.

The correction value for each nuclide was estimated in the above. In addition, the correction assuming the same corrected values for the fission and capture cross sections was carried out on the calculated ^{239}Pu and ^{241}Pu amounts, whose C/E values were overestimated as shown in Fig. 2, and their effects on the C/E ratios for ^{88,90}Sr, ^{89}Y, ^{106}Ru, ^{133,135}Cs and ^{144}Nd were also investigated. The results showed that the C/E ratios for these nuclides, except for ^{106}Ru, improved by about 2% and this trend was consistent with the trend of the correction for the fission yields discussed above. For ^{106}Ru, its calculated amount was overestimated more.

6. Effect of Power History on Nuclide Composition

To determine the effect of power history on the nuclide composition, a comparison of the nuclide compositions in the detailed[19] and constant power histories was carried out for sample A. The detailed power history is composed of 12 steps of time in each cycle. On the other hand, the constant power history as a reference case is given in Table 1. The scheme of both cases is shown in **Fig. 6**. The calculation was carried out using SWAT.

Table 19 shows the nuclides whose calculated amounts are changed more than 1% in the detailed power history. For ^{241}Am, the β^- decay of ^{241}Pu that is not sensitive to the power history predominantly affected the ^{241}Am amount during cooling. Similarly, for ^{155}Gd, the β^- decay of ^{155}Eu that is also not sensitive to the power history affected the ^{155}Gd amount during cooling. Thus, although the amounts of ^{241}Am and ^{155}Gd calculated with the detailed power history increased by 1.4 and 3.6% at discharge, respectively, their increased ratios decreased with the contribution of β^- decay during cooling. The ^{135}Cs amount is mainly

Table 19 Effects of power history on nuclide composition

Nuclide	Change in amount (%)* At discharge	After 1-year cooling	After 2-year cooling
^{241}Am	1.4	0.7	0.6
^{242m}Am	1.0	1.0	1.0
^{135}Cs	1.7	1.7	1.7
^{149}Pm	−5.1	—	—
^{149}Sm	0.2	−1.9	−1.9
^{155}Sm	−4.7	—	—
^{155}Gd	3.6	0.2	0.2

*(Amount of detailed power − Amount of constant power) × 100/(Amount of constant power)

produced through the β^- decay of ^{135}Xe whose capture cross section and half-life are 1.94×10^5 barn and 9.1 hours, respectively. The power level at the last step of the detailed power history was lower than that of the constant one, and it made the capture reaction of ^{135}Xe decrease; consequently, the ^{135}Cs amount produced from ^{135}Xe increased. In ^{149}Pm and ^{155}Sm, their half-lives, which are 2.2 days and 22.3 minutes, respectively, are slightly short. Thus, their amounts at discharge decreased, depending on the lower power level at the last step of the detailed power history. The ^{149}Pm amount also affected the ^{149}Sm amount by its β^- decay; consequently, the ^{149}Sm amount also decreased.

7. Comparison of JENDL with ENDF/B-VI, JEF and JEFF for Fission Products Showing Dependence on Type of Library

In Fig. 3, the C/E ratios for ^{154}Eu, ^{154}Gd, ^{155}Eu and ^{155}Gd strongly depend on the type of library. Thus, the reason for the dependence was investigated using the sensitivity coefficients as follows.

(1) ^{154}Eu and ^{154}Gd

The C/E ratios for ^{154}Eu and ^{154}Gd calculated with ENDF/B-VI.5 and JEF-2.2 are larger than those calculated with the other libraries. In the sensitive path for ^{154}Eu described in Section 4, the C/E ratios for the fission products from ^{151}Sm to ^{153}Eu and the capture cross sections of ^{151,152}Sm and ^{153}Eu to which the ^{154}Eu amount are sensitive are similar among the libraries. Additionally, the ^{154}Eu capture cross sections calculated with ENDF/B-VI.5 and JEF-2.2 are about 230 and 115 barn, respectively, and these values are smaller than those calculated with the other libraries (about 270 barn). The ^{154}Eu amount is also sensitive to ^{154}Eu's own capture cross section ($S = -0.83$). Thus, the overestimation of the ^{154}Eu amounts calculated with the two libraries was caused by ^{154}Eu's own small capture cross sections. Consequently, the calculated amounts of ^{154}Eu affected directly those of ^{154}Gd. Regarding ENDF/B-VI.8 and JEFF-3.0, the capture cross sections for ^{154}Eu improved, and their C/E ratios were similar to those calculated with JENDL-3.2 and JENDL-3.3.

(2) ^{155}Eu and ^{155}Gd

The main sensitive path for ^{155}Gd is from ^{155}Eu to ^{155}Gd as mentioned in Section 4. The C/E ratios for ^{155}Eu and ^{155}Gd calculated with ENDF/B-VI.5 are smaller than those calculated with the other libraries. The ^{154}Eu capture cross section calculated with ENDF/B-VI.5 is smaller than those calculated with the other libraries and the ^{155}Eu capture cross section calculated with ENDF/B-VI.5 (about 1100 barn) is larger than those in other libraries (660–780 barn). Additionally, the ^{155}Eu amount is sensitive to ^{154}Eu and ^{155}Eu's own capture cross sections. Therefore, the ^{155}Eu amount calculated with ENDF/B-VI.5 was smaller than those calculated with the other libraries and affected directly the ^{155}Gd amount. In ENDF/B-VI.8, the ^{155}Eu capture cross section was improved, so that the C/E ratio for ^{155}Eu was near 1.00.

In the calculation with JEF-2.2, the C/E ratio for ^{155}Eu is 1.09, although that for ^{154}Eu is 2.09. The ^{154}Eu capture cross section calculated with JEF-2.2 is about half those calculated with the other libraries. Thus, the C/E ratio for ^{155}Eu in JEF-2.2 improved to nearly 1.00.

IV. Conclusions

A chemical isotopic analysis of a high-burnup PWR-UO_2 fuel was carried out, followed by computational analysis using SWAT. The underestimation of the calculated ^{244}Cm amount was discussed using the simple depletion calculation, and the fission products such as ^{88}Sr, ^{90}Sr, ^{89}Y, ^{106}Ru, ^{133}Cs, ^{135}Cs and ^{144}Nd were also investigated to improve their calculated amounts using simplified burnup chains. The effect of power history on nuclide composition and the dependence of the C/E ratios for fission products on the type of library were discussed. The following results were obtained.

(1) The extensive isotopic compositions such as uranium, neptunium, plutonium, americium, curium, rubidium, strontium, yttrium, ruthenium, cesium, lanthanum, cerium, praseodymium, neodymium, promethium, samarium, europium and gadolinium of the three samples extracted at different axial positions of a high-burnup UO_2 fuel were obtained experimentally to evaluate and improve the calculation accuracy.

(2) The calculated amount of ^{244}Cm, which is the major neutron emitter in spent fuels, was significantly underestimated. From the results calculated with the adjusted capture cross sections of ^{243}Am and plutonium isotopes, the calculation accuracy of ^{244}Cm could be improved by reevaluating the capture cross sections of both ^{243}Am and plutonium isotopes.

(3) For ^{88}Sr, ^{90}Sr and ^{106}Ru, the correction for their own fis-

sion yields improved their C/E ratios. In the case of ^{89}Y, the correction for the ^{89}Sr fission yield improved the C/E ratio for ^{89}Y. For ^{133}Cs, the correction for the ^{133}Xe fission yield improved the C/E ratio for ^{133}Cs. On the other hand, for ^{135}Cs, it was suggested that the underestimation of the fission yield or the overestimation of the capture cross section of ^{135}Xe resulted mainly in the underestimation of the calculated ^{135}Cs amount. In the case of ^{144}Nd, it was suggested that the underestimation of the ^{144}Ce fission yield resulted mainly in the underestimation of the calculated ^{144}Nd amount.

(4) In the comparison of the calculated amounts with the detailed and constant power histories, the calculated amounts of ^{241}Am, ^{242m}Am, ^{135}Cs, ^{149}Pm, ^{149}Sm, ^{155}Sm and ^{155}Gd were slightly affected by the power history.

(5) For ^{154}Eu and ^{154}Gd calculated with ENDF/B-VI.5 and JEF-2.2, the overestimation of the calculated ^{154}Eu amounts resulted from ^{154}Eu's own small capture cross sections, and the calculated amount of ^{154}Gd reflected that of ^{154}Eu. For ^{155}Eu and ^{155}Gd calculated with ENDF/B-VI.5, the ^{154}Eu capture cross section was smaller than those in the other libraries. In contrast, the ^{155}Eu capture cross section was larger than those in the other libraries. Thus, the calculated ^{155}Eu amount was smaller than those in the other libraries, and the calculated amount of ^{155}Gd directly reflected that of ^{155}Eu.

Futher experimental determination of nuclide composition is required to improve the calculation accuracy for the nuclide composition of a high-burnup UO_2 spent fuel, particularly ^{237}Np, ^{242m}Am and ^{242}Cm for actinides. For ^{241}Am, it is necessary to evaluate its calculation accuracy. Regarding fission products, it is necessary to evaluate the calculation accuracy for the amounts of ^{144}Ce, ^{147}Pm, ^{151}Sm and gadolinium isotopes, which are used as burnup indicators or contribute to neutron absorption.

Acknowledgement

The chemical isotopic analysis in this study was carried out under a contract from the Ministry of Economy, Trade and Industry (METI) of the Japanese government.

References

1) K. Suyama, A. Nouri, H. Mochizuki *et al.*, "Improvements to SFCOMPO—A database on isotopic composition of spent nuclear fuel," *Proc. 7th Int. Conf. on Nuclear Criticality Safety (ICNC2003)*, Tokai-mura, Japan, Oct. 20–24, 2003, JAERI-Conf 2003-019, Japan Atomic Energy Research Institute, 890–892 (2003).
2) K. Okumura, S. Ohki, M. Yamamoto *et al.*, *Study on the Prediction Accuracy of Nuclide Generation and Depletion with JENDL*, JAERI-Research 2004-025, Japan Atomic Energy Research Institute, (2005), [in Japanese].
3) Y. Nakahara, K. Suyama, T. Suzaki, *Technical Development on Burn-up Credit for Spent LWR Fuels*, JAERI-Tech 2000-071, Japan Atomic Energy Research Institute, (2000), [in Japanese].
4) B. D. Murphy, R. T. Primm III, "Simulation of mixed-oxide and low-enriched uranium fuel burnup in a pressurized water reactor and validation against destructive analysis results," *Nuclear Science and Engineering*, **142**, 258–269 (2002).
5) Y. Ando, K. Yoshioka, I. Mitsuhashi *et al.*, "Development and verification of Monte Carlo burnup calculation system," *Proc. 7th Int. Conf. on Nuclear Criticality Safety (ICNC2003)*, Tokai-mura, Japan, Oct. 20–24, 2003, JAERI-Conf 2003-019, Japan Atomic Energy Research Institute, 494–499 (2003).
6) A. Sasahara, T. Matsumura, G. Nicolaou *et al.*, "Neutron and gamma ray source evaluation of LWR high burn-up UO_2 and MOX spent fuels," *J. Nucl. Sci. Technol.*, **41**, 448 (2004).
7) K. Suyama, T. Kiyosumi, H. Mochizuki, *Revised SWAT—The Integrated Burn-up Calculation Code System*, JAERI-Data/Code 2000-027, Japan Atomic Energy Research Institute (JAERI), (2000), [in Japanese].
8) T. Nakagawa, K. Shibata, S. Chiba *et al.*, "Japanese Evaluated Nuclear Data Library Version 3 Revision-2: JENDL-3.2," *J. Nucl. Sci. Technol.*, **32**, 1259 (1995).
9) K. Shibata, T. Kawano, T. Nakagawa *et al.*, "Japanese Evaluated Nuclear Data Library Version 3 Revision-3: JENDL-3.3," *J. Nucl. Sci. Technol.*, **39**, 1125 (2002).
10) P. F. Rose, ENDF-201, ENDF/B-VI Summary Documentation, BNL-NCS-17541, 4th Edition, Brookhaven National Laboratory (BNL), (1991).
11) C. Nordborg, M. Salvatores, "Status of the JEF Evaluated Data Library," *Proc. Int. Conf. Nuclear Data for Science and Technology*, Gatlinburg, Tennessee, USA, May 9–13, 1994, Vol. 2, 680 (1994).
12) R. Jacqmin, R. Forrest, J. Rowlands *et al.*, "Status of the JEFF-3 Project," *Proc. Int. Conf. on Nuclear Data for Science and Technology*, Tsukuba, Japan, Oct. 7–12, 2001, Vol. 1, 54 (2002).
13) A. Sasahara, T. Matsumura, G. Nicolaou, *Posit Irradiation Examinations and the Validity of Computational Analysis for High Burn-up UO_2 and MOX Spent Fuels*, CRIEPI report, T95012, (1996), [in Japanese].
14) K. Tsuchihashi, Y. Ishigro, K. Kaneko *et al.*, *Revised SRAC Code System*, JAERI 1302, Japan Atomic Energy Research Institute, (1986).
15) A. G. Croff, *A User's Manual for the ORIGEN2 Computer Code*, ORNL/TM-7175, Oak Ridge National Laboratory, (1980).
16) K. Tasaka, J. Katakura, H. Ihara *et al.*, *JNDC Nuclear Data Library of Fission Products—Second Version—*, JAERI 1320, Japan Atomic Energy Research Institute, (1990).
17) K. Kobayashi, *Reactor Physics*, Corona Publishing Co., Ltd., (1996), [in Japanese].
18) M. Ohta, S. Nakamura, H. Harada, "Measurement of effective capture cross section of Americium-243 for thermal neutrons," *J. Nucl. Sci. Technol.*, **43**, 1441 (2006).
19) R. Bodmer, private communication (2007).